Journal of Petroleum Research and Studies

journal homepage: https://jprs.gov.iq/index.php/jprs/

Print ISSN 2220-5381, Online ISSN 2710-1096

Reservoir Characterization and Petrophysical Evaluation for Paleogene Khurmala Formation in Northern Iraq

Rzger A. Abdula[1*], Ayub M. A. Shwani[2], Parween R. Abid[1], Bienfait K. Simisi[3]

[1]Department of Petroleum Geosciences, Soran University, PO Box 624, KRG, 44008, Iraq
[2]Geology Department, Field Division, North Oil Company, Kirkuk, 36001, Iraq
[3]Geology Department, Université de la Conservation de la Nature et du Développement de Kasugho, 86CF+4JM, Goma, Democratic Republic of the Congo – Kinshasa
[*]Corresponding Author E-mail: rzger.abdula@soran.edu.iq

Article Info

Received 23/04/2025
Revised 21/07/2025
Accepted 13/08/2025
Published 21/12/2025

DOI:
http://doi.org/10.52716/jprs.v15i4.1108

Abstract

This study presents a detailed reservoir characterization and petrophysical evaluation of the Paleogene Khurmala Formation within the X Oilfield, northern Iraq. The analysis is based on digitized well log data, including density, neutron porosity, gamma ray, and resistivity logs, processed using Neuralog and Techlog 2018 software. Lithology was determined through neutron-density cross plots, confirming the presence of heterogeneous carbonate sequences consisting of dolomite and limestone. Shale volume was calculated using gamma ray logs, revealing localized shale enrichment in parts of the formation. Effective porosity was derived by correcting density and neutron porosity logs for shale influence, while permeability was estimated through porosity-permeability relationships. Water saturation was calculated using Archie's equation, indicating that large portions of the formation are water-saturated with low hydrocarbon potential, except for one zone (RU-3) which demonstrates favorable reservoir characteristics. The formation was divided into four reservoir units based on variations in shale content, porosity, water saturation, and permeability. RU-3 exhibited the best petrophysical properties, with high porosity, low water saturation, and minimal shale content, making it the most promising target for hydrocarbon production. The results provide valuable insights for optimizing reservoir management in this field.

Keywords: Khurmala Formation, Reservoir Characterization, Porosity, Permeability, Hydrocarbon potential.

توصيف المكمن والتقييم البتروفيزيائي لتكوين خورمالة من عصر الباليوجين في شمال العراق

الخلاصة:

تقدم هذه الدراسة توصيفاً دقيقاً للمكمن وتقييماً بتروفيزيائياً لتكوين خورمالة من عصر الباليوجين ضمن حقل X النفطي في شمال العراق. استند التحليل إلى بيانات مجسات الآبار الرقمية، والتي شملت مجسات الكثافة، المسامية النيوترونية، أشعة غاما، والمقاومية، وتمت معالجتها باستخدام برامج Neuralog و Techlog 2018 المتخصصة. تم تحديد التكوين الصخري من خلال مخططات التقاطع بين مسامية النيوترون والكثافة، والتي أكدت وجود تتابعات كربوناتية غير متجانسة تتكوّن من الدولوميت والحجر الجيري. تم حساب حجم الطين باستخدام مجسات أشعة غاما، والتي أظهرت وجود تراكمات موضعية للطين في بعض أجزاء التكوين. كما تم حساب المسامية الفعالة بعد تصحيح قراءات مسامية النيوترون والكثافة لتأثير الطين، بينما تم تقدير النفاذية من خلال علاقات تجريبية تربط بين المسامية والنفاذية. تم حساب تشبع الماء باستخدام معادلة آرشي (Archie's equation)، وأظهرت النتائج أن معظم أجزاء التكوين مشبعة بالماء مع انخفاض في احتمالية وجود الهيدروكربونات، باستثناء منطقة واحدة (RU-3) التي أظهرت خصائص مكمنية جيدة. تم تقسيم التكوين إلى أربع وحدات مكمنية بناءً على التغيرات في محتوى الطين، المسامية، تشبع الماء، والنفاذية. أظهرت الوحدة الثالثة (RU-3) أفضل الخصائص البتروفيزيائية من حيث ارتفاع المسامية، انخفاض تشبع الماء، وانخفاض محتوى الطين، مما يجعلها الوحدة الأكثر واعداً لإنتاج الهيدروكربونات. توفر هذه النتائج معلومات قيّمة تساعد في تحسين إدارة المكمن وتطوير الإنتاج في هذا الحقل.

1. Introduction

The Paleogene Khurmala Formation holds considerable economic importance as it serves as a hydrocarbon reservoir in several oil fields across northern Iraq [1]. The formation was first described by [2]. at its type locality in well Kirkuk-114, where it is predominantly composed of dolomite—partly exhibiting pseudo plastic textures—and finely recrystallized limestone. The Khurmala Formation consists of limestone and dolomite [1], [2], [3], [4]. Built on outcrop indications and petrographic investigation, the Khurmala Formation is deposited in a shallow marine environment [5], [6], [7].

Several studies have investigated the Khurmala Formation with respect to its hydrocarbon potential and reservoir properties in northern Iraq. Studies in early works shed light on the depositional settings and lithological variability of the formation, which are essential for understanding reservoir distribution [3], [8]. More recent investigations emphasized sedimentological controls, diagenetic processes, and microfacies development that influence reservoir quality [1], [9], [10]. Petroleum-oriented research further highlighted the heterogeneous character of the Khurmala Formation, marked by interbedded dolomite and limestone with variable porosity and permeability [11], [6], [5], [12]. These works also demonstrated that fracture networks and vuggy porosity may enhance reservoir performance in localized zones.

The primary aim of this research is to describe reservoir characterization of the Khurmala Formation in the X Field. This involves analyzing the formation's petrophysical properties, e.g., lithology, shale volume, porosity, and fracture identification, to evaluate its reservoir potential and quality. Considering these characteristics is vital for actual reservoir management and optimization of hydrocarbon recovery.

1.1 Cenozoic History

After the end of the Upper Cretaceous Epoch, Tertiary facies were deposited unconformably over the Shiranish Formation [13]. The Tertiary Period witnessed the development of the Sinjar Belt, extending across northern Iraq, including the Khurmala Dome. This structural feature, attributed to Alpine Orogeny, played a significant role in shaping the sedimentary basin and influenced the deposition and preservation of the Khurmala Formation carbonates [13], [14].

The progressive shallowing of the Sinjar Shelf due to tectonic uplift resulted in the development of shoal and reefal facies, including the coral-rich Khurmala Formation, deposited during the Paleocene to early Eocene [9]. These shallow marine carbonates are characterized by dolomite and limestone sequences, which form the primary reservoir units in the region.

Uplift and erosion during subsequent geological periods exposed the Khurmala area, affecting reservoir preservation and diagenetic processes such as dolomitization and fracturing, which are critical to understanding its reservoir quality today.

2. Methods

The materials and methods of this study are based on the analysis and interpretation of well log data to evaluate the reservoir properties of the subsurface section in the X Oilfield.

This study relied on the use of specialized software for data processing and interpretation, including Neuralog for digitizing well logs and Techlog 2018 for petrophysical analysis. The dataset used in this study was obtained by digitizing three key well logs: density, neutron porosity, and gamma ray logs, which were employed to assess the petrophysical characteristics of the Khurmala Formation. The integration of these well log analyses, along with geological information, contributed to a better understanding of the reservoir's structural framework and hydrocarbon potential, thus supporting exploration and development activities within the X Oilfield.

3. Results and Discussion

3.1. Lithology description

The formation consists of oolitic dolomite and recrystallized limestone [15]. A detailed petrographic analysis of a dolomitic limestone sequence in the Darbandikhan area within the Sulaymaniyah region was previously reported [5]. Further investigations of the Khurmala Formation in the Tawke and Shaqlawa areas indicate that it is primarily composed of limestone,

dolomite, and dolomitic limestone [16]. Overall, the lithology of the Khurmala Formation appears to represent a homogeneous rock unit, as illustrated in Figures (1) and (2).

3.2. Shale Volume Determination

The shale content within the Khurmala Formation was estimated using gamma-ray logs, which serve as a primary indicator due to the higher concentrations of radioactive elements found in shales. Therefore, gamma-ray logs provide a good indicator of shale content [17], which is given by formulas (1 & 2):

$$I_{gr}=\frac{(Grlog-Grmin)}{(Grmax-Grmin)} \quad \ldots\ldots\ldots\ldots\ldots\ldots\ldots\ldots (1)$$

$$Vsh = 0.83\ x\ (2^{3.7}\ x\ Igr - 1 \quad \ldots\ldots\ldots\ldots (2)$$

The calculated shale volume indicates variability across the formation. According to Ghorab et al. [18], shale content is classified as follows:

Less than 10%: Clean zone

10% to 35%: Shaly zone

Greater than 35%: Shale zone

In this context, an interval around 1130 m depth exhibited gamma-ray values corresponding to a shale content exceeding 35%, suggesting localized shale enrichment within the carbonate succession. However, it is important to note that in carbonate-dominated formations, elevated gamma-ray readings may also be influenced by the presence of radioactive minerals within the carbonate matrix itself, rather than pure shale layers, (Figure 3).

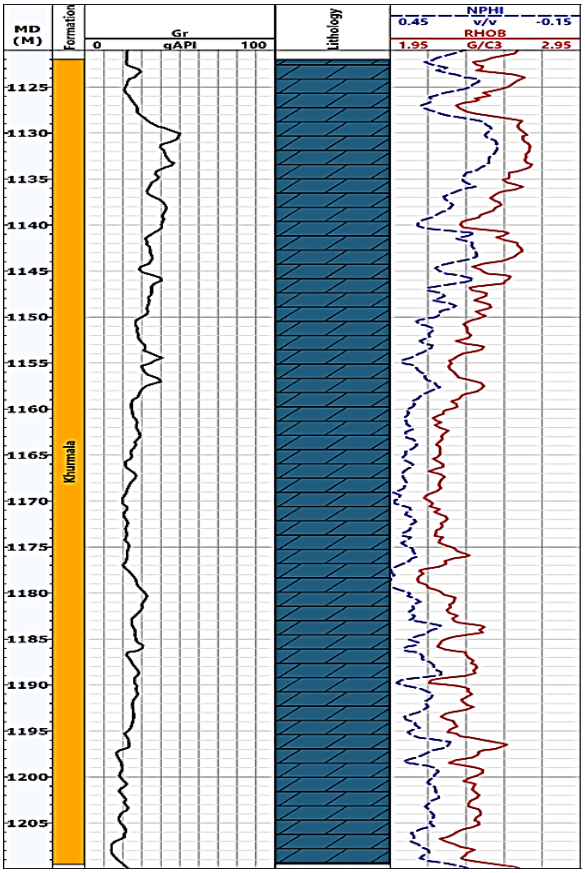

Fig. (1): Graphic well log for studied well.

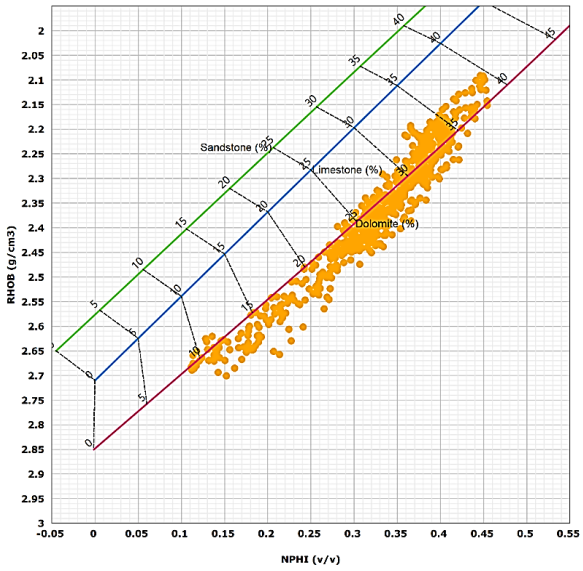

Fig. (2): Detection lithology by cross plot of neutron porosity versus density porosity.

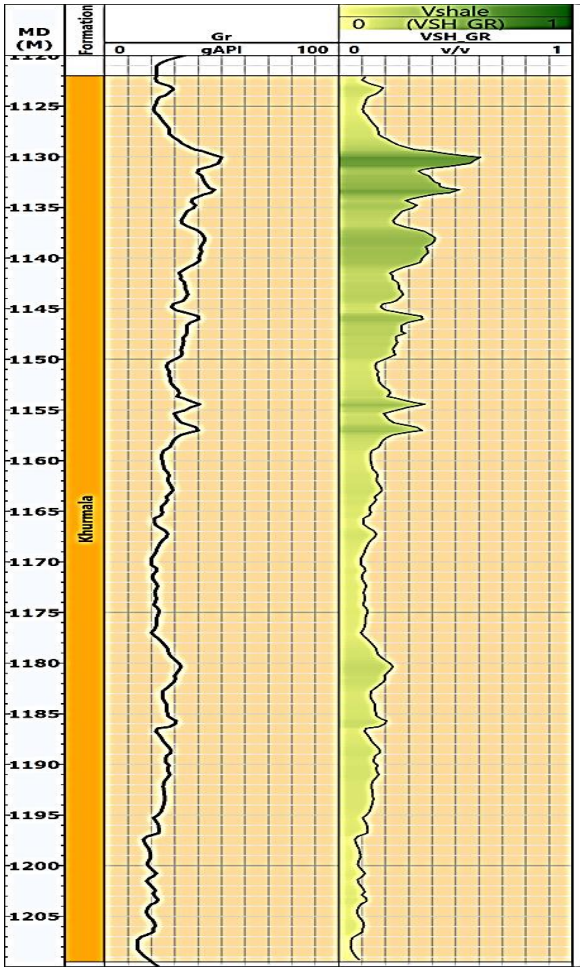

Fig. (3): Natural Gamma ray and Shale volume curve.

3.3. Effective Porosity Determination

3.3.1. Density log

The density log contains a radioactive source and two detectors and can be used quantitatively to calculate porosity and to determine indirectly the hydrocarbon density. Qualitatively, it is suitable as a lithology indicator, minerals' recognizer, organic source rock evaluation, and abnormal pressure and fracture porosity identifier [19]. Porosity classifications provide insight into the storage capacity of reservoir rocks. To evaluate porosity, the qualitative description of North [20] was applied (Table 1). the formula (3) used to calculate porosity from the density tool:

$$PHIT\_D=\frac{(Pma-Plog)}{(Pma-Pfl)} \quad \ldots\ldots\ldots\ldots\ldots\ldots\ldots\ldots (3)$$

PHIT_D: density derived porosity

P_{ma}: matrix density

P_{log}: log reading, gm/cm^3

P_{fl}: density fluid

Table (1): The porosity ranges are categorized as follows (according to North [20]).

Description	Porosity (%)
Negligible	0-5
Poor	5-15
Good	15-20
Very good	20-30
Excellent	>30

3.3.2. Neutron porosity

Neutron logs are porosity logs that accounting the hydrogen absorption exist in the pore spaces within the reservoir formation. These logs effectively measuring those porosities filled liquids [21]. This porosity value can be obtained directly from neutron tool reading [22]. The porosity value calculated from neutron and density logs must be cleaned from shale content by the following equations:

$$PHIE\_D = PHIT\_D - (Vsh\ x\ PHID\_sh \ldots\ldots\ldots (4)$$

$$PHIE\_N = PHIT\_N - (Vsh\ x\ PHIN\_sh \ldots\ldots\ldots (5)$$

PHIE_D: effective density porosity

PHIT_N: from tool reading

PHIE_N: effective neutron porosity

V_{sh}: volume of shale

PHID_Sh: density porosity from adjacent of shale

PHIN_Sh: neutron porosity from adjacent of shale

The neutron-density combination log, based on the Schlumberger [23], provides a way to calculate total effective porosity PHIE_ND both before and after making corrections for shale impact.

$$\text{PHIE\_ND} = \frac{(\text{PHIE\_D} + \text{PHIE\_N})}{2}$$

The fracture and vuggy porosity distributions in the given well log vary with depth (Figure 4).

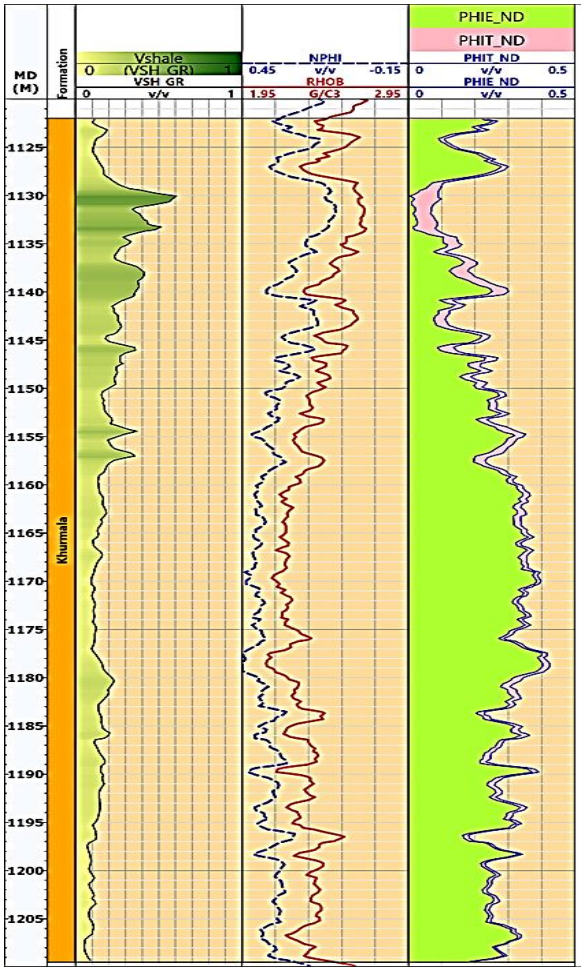

Fig. (4): Corrected and uncorrected total porosity with shale volume.

The fracture and vuggy porosity distributions in the given well log vary with depth (Fig. 4). In the upper interval (1125–1155 m), minimal separation is observed between the neutron and density porosity logs, with no significant neutron-density crossover present. Therefore, the presence of natural fractures cannot be confirmed solely based on the available log data. Additional direct evidence, such as borehole image logs or core samples, would be required to accurately identify fracture development in this interval. Within the Khurmala Formation (1155–1185 m), more pronounced neutron-density separation is noted, which may suggest enhanced porosity; however, further investigation is necessary to differentiate between true vuggy porosity, fractures, or lithological effects. In the deeper section (1185–1205 m), irregular porosity fluctuations and limited neutron-density separation are observed, but without direct geological evidence, fracture presence remains inconclusive. The final effective porosity (PHIE_ND) was derived by averaging the corrected neutron and density porosity values, with adjustments made to account for shale content based on gamma-ray log interpretation (Vsh). Applying these corrections is essential in

carbonate reservoirs like the Khurmala Formation, where lithological heterogeneity and shale distribution can significantly distort porosity readings.

To enhance reservoir evaluation, the effective porosity results were integrated with other datasets, including gamma-ray profiles and lithological indicators. Zones characterized by higher effective porosity were found to correlate with clean carbonate intervals containing minimal shale.

3.4. Permeability

Permeability refers to the capacity of rocks to diffuse liquids, typically measured in units called Darcy or milliDarcy. For a rock to be permeable, it must have interconnected pores [24]. The permeability distribution across the Khurmala Formation in the provided log varies with depth (Figure 5).

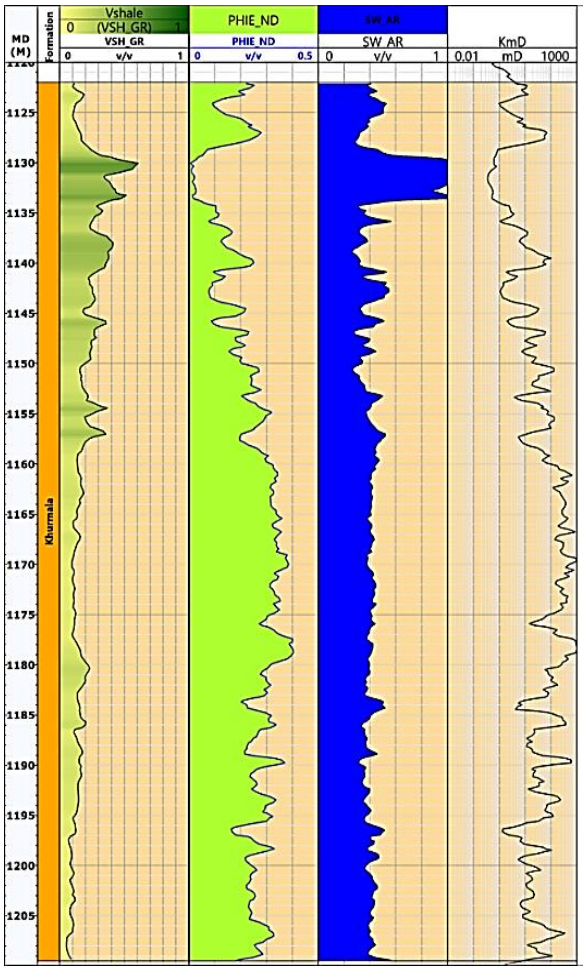

Fig. (5): Predicted and core permeability curve with porosity and gamma ray logs.

Between 1125–1155 m, permeability is very low (<0.1 mD), indicating a tight formation with minimal fluid flow potential; between 1155–1185 m, the permeability is slightly higher in some

intervals (0.1–1.0 mD) due to possibility of existing minor fractures or better reservoir quality zones; between 1185–1205 m, the permeability is moderate with some peaks reaching a few mD, suggesting localized fracture influence, but still generally low matrix permeability. The Khurmala Formation exhibits predominantly low permeability with minor improvements in certain depth intervals, likely due to natural fractures.

Permeability was predicted using an empirical relationship between porosity and permeability, commonly applied in carbonate reservoir studies. The following equation was used:

$K = a\ x\ (\text{PHIE\_ND})^b$

Where

K is permeability in millidarcies.

PHIE_ND is the corrected effective porosity.

a and *b* are formation-specific constants.

The relationship between porosity and permeability shows a positive correlation, as seen in the cross-plot (Figure 6), where permeability increases significantly above a porosity threshold of approximately 7% (0.07 v/v). This threshold corresponds to the cut-off for effective reservoir quality.

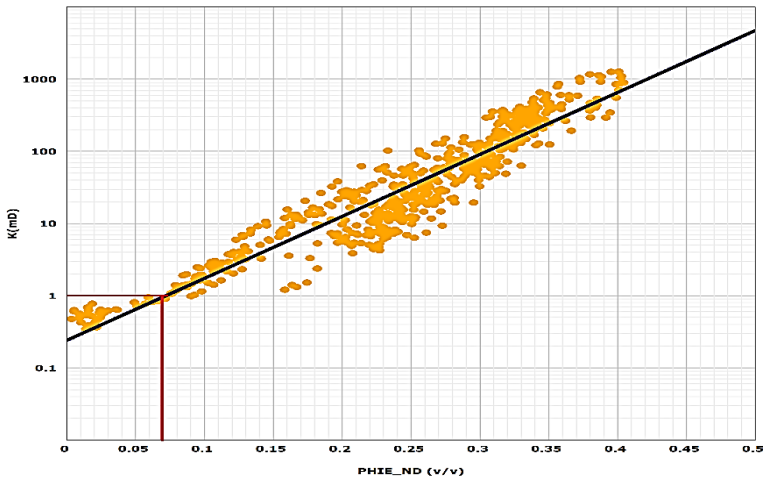

Fig. (6): Permeability against porosity for the Khurmala Formation.

Furthermore, available core data from neighboring fields indicate similar permeability trends, supporting the reliability of the predicted values. By integrating porosity, permeability, and shale volume data, the reservoir zones can be better evaluated, with RU-3 emerging as the most promising interval due to its high porosity and moderate permeability peaks, indicating enhanced fluid flow potential.

3.5. Water saturation

Water saturation refers to the spaces in a reservoir rock that equipped by water. Archie's equation, which was formulated in 1942 [21] can be applied to calculate it. The formula is:

$$K = Sqrt(\frac{(A\ x\ Rw)}{(Rt\ x\ \text{PHIE\_ND})^m}) \dots\dots\dots\dots\dots\dots\dots\dots\dots (6)$$

The water saturation (S_w) log of the Khurmala Formation indicates that the formation is predominantly water-saturated throughout the depth interval from 1130 m to 1205 m. The S_w values remain consistently high, close to 1.0 (100%), suggesting that the pore spaces are entirely filled with water, with no significant hydrocarbon presence.

In the depth interval 1130 m to 1135 m, the water saturation (S_w) log indicates high values, close to 1.0 (100%), suggesting that this zone is fully water-saturated. There is no significant reduction in S_w, meaning there is no indication of hydrocarbon presence in this interval. This further supports the interpretation that the Khurmala Formation is water-bearing rather than a productive hydrocarbon reservoir.

In the depth interval 1135 m to 1205 m, the water saturation (S_w) log remains consistently high, close to 1.0 (100%), indicating that the pore spaces are completely filled with water. There are no noticeable decreases in S_w that would suggest hydrocarbon accumulation. This uniform high saturation confirms that this section of the Khurmala Formation is fully water-bearing, with no indications of hydrocarbon presence.

Given the low permeability observed in this formation, it is likely composed of tight carbonates (limestones or dolomites), further limiting hydrocarbon migration and retention. Therefore, this interval behaves as an aquifer rather than a hydrocarbon reservoir (Figure 7).

3.6. Reservoir Units

The evaluation of the Khurmala Formation in this well suggests that hydrocarbon productivity is limited. RU-3 in the Khurmala Formation stands out as the best reservoir based on well log analysis and petrophysical properties. It demonstrates the highest effective porosity (PHIE_ND), indicating excellent storage capacity for hydrocarbons. The low water saturation (S_W_AR) suggests that the pore spaces are predominantly filled with hydrocarbons, rather than water.

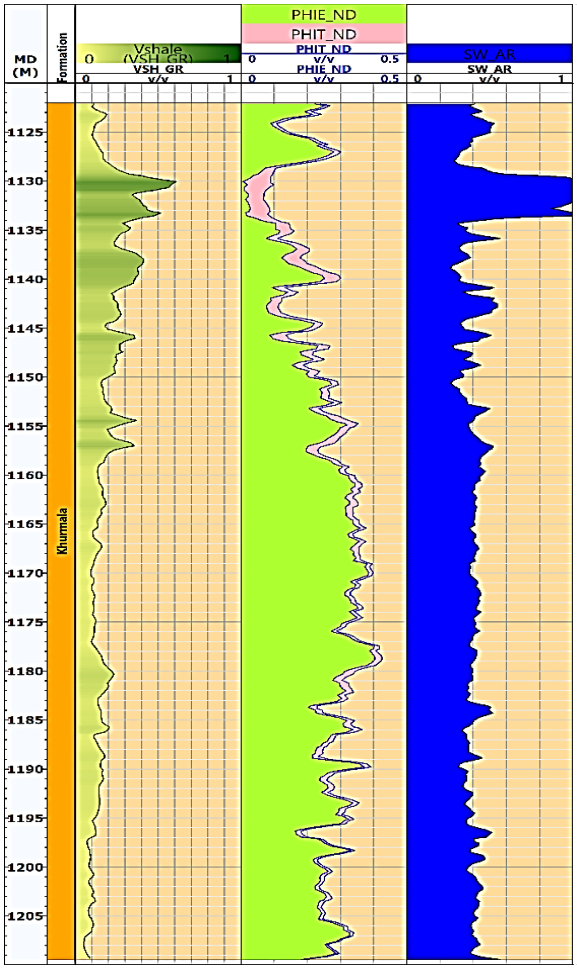

Fig. (7): Moved and residual hydrocarbon with saturation water.

Additionally, the minimal shale volume (V_{sh} GR) highlights a clean reservoir rock, which enhances permeability. The significant density-neutron cross-over (RHOB & NPHI) is a classic indicator of gas-bearing zones, further supporting its hydrocarbon potential. With a gross thickness of 18.2 meters, RU-3 provides a substantial hydrocarbon-bearing interval, characterized by high porosity, low shale content, and low water saturation. These factors make RU3 the most favorable target for hydrocarbon production in the Khurmala Formation (Figure 8).

3.7. Cut off parameters

The net reservoir determination is not easy, and it is a complex in fractured zones associated with matrix porosity, because very low permeability rock may be feeding the fracture system, and therefore producing a cut-off based on matrix permeability NTG=IF PHIE_ND>=0.07, IF S_w<=0.5, IF V_{SH}<=0.4.

The cut-off analysis for the Khurmala Formation is based on the relationship between effective porosity (PHIE_ND), permeability (K) (Fig. 6), and water saturation (S_w) (Fig. 9).

The permeability versus porosity cross-plot shows a strong correlation, indicating that permeability increases with porosity. A cut-off porosity value of approximately 0.07 v/v (7%) is evident, below which permeability drops below 1 mD, marking the lower limit for effective reservoir quality. Similarly, in the water saturation against porosity diagram, water saturation remains high above the cut-off porosity, confirming that lower porosity zones are water-saturated and non-productive. Therefore, intervals with PHIE_ND below 7% are unlikely to contribute to hydrocarbon production, while zones exceeding this threshold exhibit favorable reservoir characteristics.

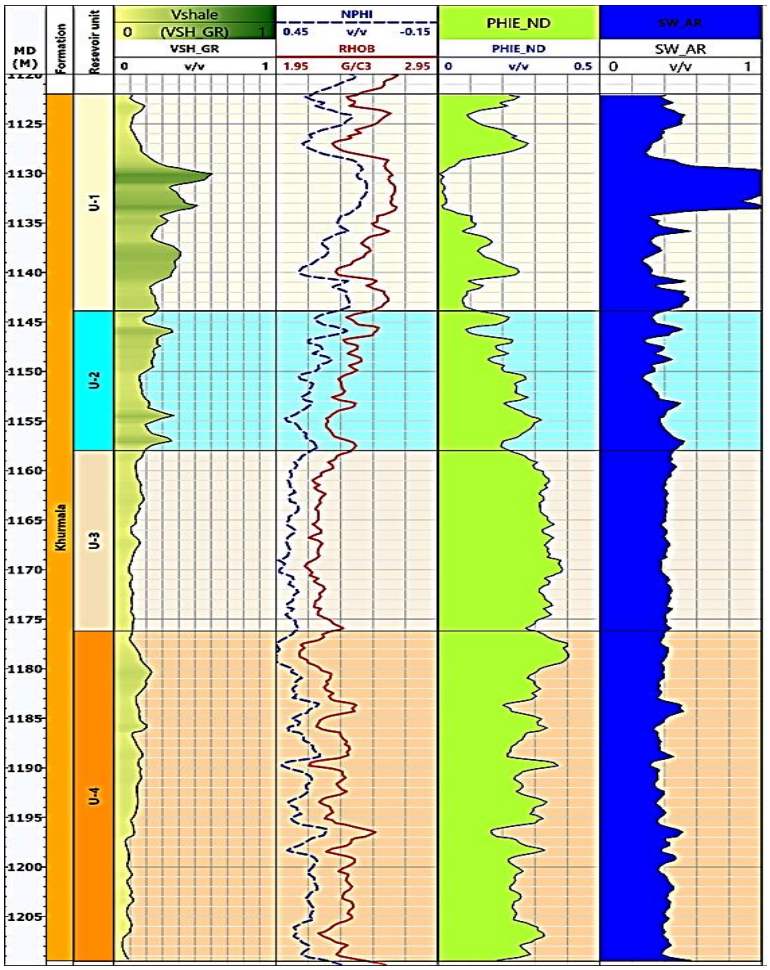

Fig. (8): Reservoir units (RU-1 to RU-4) of the Khurmala Formation based on well log interpretation.

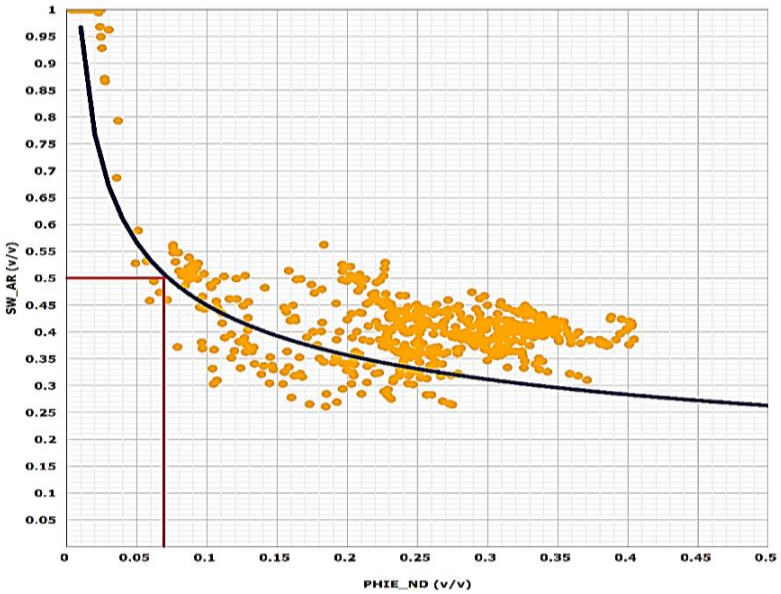

Fig. (9): Water saturation against porosity for the Khurmala Formation.

4. Discussion

Discussion of well log analysis came after calculating the various petrophysical properties of the reservoir rock. The Khurmala Formation in this study well divided into four reservoir units depending on variations in shale volume content, total effective porosity, water saturation, and permeability (Figure 8). To calculate and detect various parameters such as the gross thickness of the reservoir, the net to gross and pay ratios of the reservoir, Table (2) and Figure (10) help detect the location of the best expected productive reservoir units for oil within the reservoir.

Table. (2): Determination Gross, Net, N/G, Av. Vsh, Av. PHIE_ND, Av. S_w and Av. KmD.

Well	Formation	Reservoir unit	Flag Name	Top	Bottom	Gross (M)	Net (M)	Net to Gross	BVW (M)	Av_Shale Volume (v/v)	Av_Porosity (v/v)	Av_Water Saturation (v/v)
K-K	Khurmala	U-1	Rock	1122	1144	21.885	17.802	0.813	0.982	0.247	0.142	0.388
			Res	1122	1144	21.885	15.667	0.716	0.930	0.233	0.156	0.379
			Pay	1122	1144	21.885	12.927	0.591	0.802	0.237	0.171	0.363
		U-2	Rock	1144	1158	14.076	14.076	1.000	1.171	0.238	0.219	0.381
			Res	1144	1158	14.076	14.076	1.000	1.171	0.238	0.219	0.381
			Pay	1144	1158	14.076	13.467	0.957	1.117	0.234	0.221	0.376
		U-3	Rock	1158	1176	18.214	18.214	1.000	2.491	0.132	0.328	0.416
			Res	1158	1176	18.214	18.214	1.000	2.491	0.132	0.328	0.416
			Pay	1158	1176	18.214	18.214	1.000	2.491	0.132	0.328	0.416
		U-4	Rock	1176	1210	33.325	33.325	1.000	3.692	0.128	0.279	0.397
			Res	1176	1210	33.325	33.325	1.000	3.692	0.128	0.279	0.397
			Pay	1176	1210	33.325	32.356	0.971	3.589	0.127	0.281	0.394

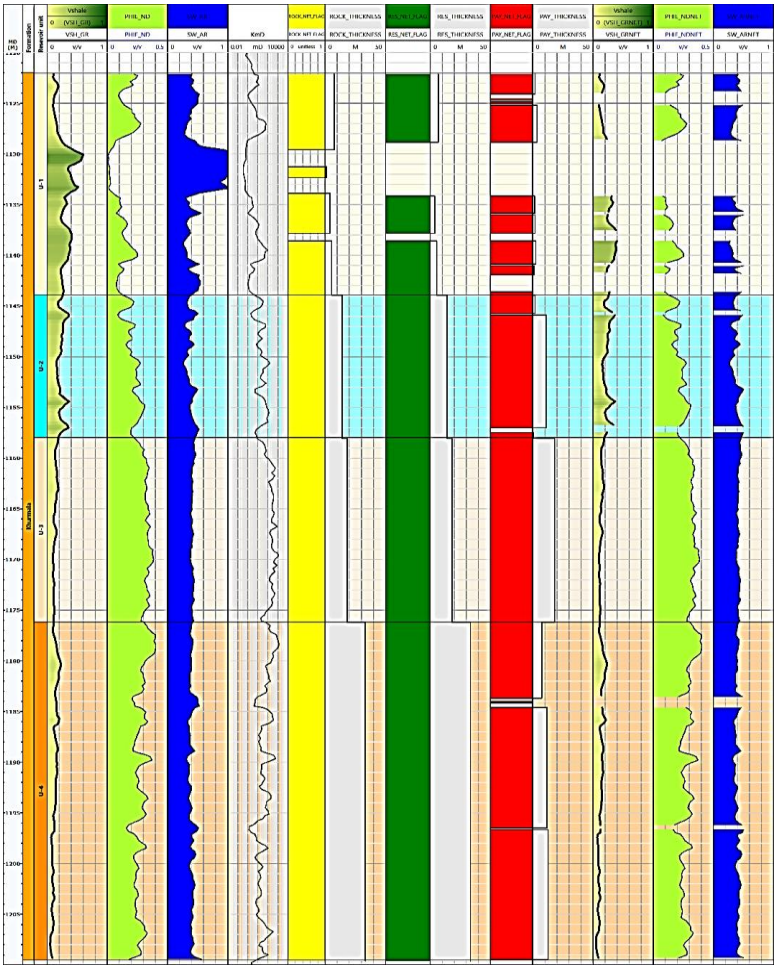

Fig. (10): Techlog processing interpretation showing Rock, Reservoir, and Pay thicknesses.

Reservoir RU-3 represents the third reservoir in the studied well with a thickness of 18.2 m based on its excellent petrophysical properties. This unit exhibits the highest porosity (0.328 v/v), the lowest shale volume (0.132 v/v), and the lowest water saturation (0.317 v/v) among all four units. These characteristics make Unit 3 the most effective hydrocarbon-bearing interval, ensuring better fluid flow and higher recoverable reserves.

Additionally, the high net-to-gross ratio in this unit indicates that most of its thickness consists of clean, productive reservoir rock rather than non-reservoir material. The lower water saturation further confirms that hydrocarbons are the dominant fluid, reducing the risk of water production and enhancing overall recovery efficiency.

RU-4 also shows good reservoir characteristics, but its slightly higher water saturation (0.394 v/v) could lead to water production challenges. RU-1 and RU-2 have moderate reservoir properties, but they do not match the superior characteristics of RU-3.

5. Conclusions

This study provides a comprehensive evaluation of the Khurmala Formation in northern Iraq, utilizing well-log data to determine its petrophysical properties and reservoir potential. The formation is primarily composed of dolomite with localized limestone occurrences, exhibiting variable porosity and low permeability. Shale volume analysis indicates a mix of clean and shaly zones, while water saturation results suggest that much of the formation is water-bearing, reducing its hydrocarbon prospectivity. Among the four identified reservoir units, RU-3 emerges as the most promising, featuring the highest effective porosity, the lowest shale volume, and the lowest water saturation. However, the overall low permeability and high water saturation in many intervals present challenges for hydrocarbon recovery. The results highlight the significance of fracture networks in improving reservoir value and suggest that future development efforts should focus on optimizing production from the most favorable reservoir units while considering advanced recovery techniques.

Author Contributions Statement: Rzger A. Abdula contributed to the conception of the research, research design, drafting of the manuscript, and revision and proofreading of the manuscript. Ayub M. A. Shwani contributed to the data processing and analysis. Parween R. Abid contributed to the data interpretation and literature review. Bienfait K. Simisi contributed to the revision and proofreading of the manuscript. All authors have read and approved the final version of the manuscript.

References

[1] M. M. Al-Dabagh, "Facies and depositional model of Khurmala Formation (Paleocene-Early Eocene) at selected exposures from northern Iraq", *Unpublished MSc. Thesis, Mosul University*, Iraq (in Arabic), 114p., 2010.

[2] R. C. Van Bellen, H. V. Dunnigton, R. Wetzal, and D. M Morton, "Lexique Stratigraphique International", V. III, 333p., *Paris, Centre Recherche Scientifique, Internat. Geol Cong Comm Stratigr,* 1959.

[3] B. Al-Qayim, "Sedimentary facies anatomy of Khurmala Formation, northern Iraq", *Iraqi Geological Journal*, vol. 28**,** no. 1, pp. 36-46, 1995.

[4] B. Al Qayim, A. Omer, and H. Koyi, "Tectonostratigraphic overview of the Zagros suture zone, Kurdistan region, northeast Iraq", *GeoArabia*, vol. 17, no. 4, pp. 109-156, 2012. https://doi.org/10.2113/geoarabia1704109

[5] K. H. Karim, H. S. Daoud, and A. R. Kuradawy, "Record of Khurmala Formation (Late Paleocene–Early Eocene) in the Sulaimaniyah governorate, Kurdistan region, northeast Iraq", *Iraqi Geological Journal*, vol. 51, no. 1, pp. 34-55, 2018. https://doi.org/10.46717/igj.51.1.3Ms-2018-06-25

[6] I. S. Asaad, and S. M. Balaky, "Microfacies analysis and depositional environment of Khurmala Formation (Paleocene–Lower Eocene), in the Zenta village, Aqra district, Kurdistan region, Iraq", *Iraqi Bulletin of Geology and Mining*, vol. 14, no. 2, pp. 1-15, 2018.

[7] I. S. Asaad, M. A. Al-Haj, and Z. A. Malak, "Depositional setting of Khurmala Formation (Paleocene-Early Eocene) in Nerwa section, Berat Anticline, Kurdistan Region, Northern Iraq", *Iraqi Geological Journal*, vol. 55, no. 1F, pp. 20-39, 2022. https://doi.org/10.46717/igj.55.1F.2Ms-2022-06-17

[8] S. I. Al-Sakry, "Sequence stratigraphy of the Paleocene – Lower Eocene succession, northeastern Iraq", *Unpublished Ph.D. Thesis, Baghdad University, Iraq*, 240p, 2006.

[9] Ch. A. Karim, "Stratigraphical and paleontological study of Khurmala Formation (Paleocene – Lower Eocene) in Shaqlawa Area -Northern Iraq", *Unpublished MSc. Thesis, Mosul University, Iraq*, 103p, 2009.

[10] N. M. Salih, "Stratigraphy and paleoenvironment of the Khurmala and Sinjar formations at Shira Swar, Shinawa and Bekhme in Kurdistan Region, Northeastern Iraq", *Unpublished M.Sc. Thesis, Erbil, University of Salahaddin-Erbil*, 157p, 2010.

[11] M. Y. Tamar-Agha, A. L. Salih, A. A. Al-Zaidy, 2015. Depositional setting and basin development of the Paleocene—Lower Eocene Sinjar and Khurmala formations, Northern Iraq", *Arabian Journal of Geosciences*, vol. 8, no. 11, pp. 9441-9467. https://doi.org/10.1007/s12517-015-1871-y

[12] A. Barzani, "Lithostratigraphy and microfacies analysis of the Khurmala Formation, Duhok Area, Kurdistan region, Iraq", *MSc. Thesis, University of Sulaimani, Iraq*, 113p, 2020.

[13] S.Z. Jassim and T. Buday, 2006. Middle Palaeocene-Eocene Megasequence AP10, chapter 13, in: S.Z. Jassim and J.C. Goff (eds.), "Geology of Iraq", first edition: *Brno, Czech Republic, Prague and Moravian Museum*, pp. 205-227, 2006.

[14] P. R. Sharland, D. M. Casey, R. B. Davies, M. D. Simmons, and O. E. Sutcliffe, "Arabian plate sequence stratigraphy–revisions to SP2", *GeoArabia*, vol. 9, no. 1, pp. 199-214, 2004.

[15] T. Buday, "The Regional Geology of Iraq" Vol. 1, Stratigraphy and paleogeography. *Dar Al-Kutub Publication University of Mosul, Iraq*, 445p, 1980.

[16] R. A. Abdula, H. S. Hussein, M. S. Hamad, and A. M. Abdulla, "Reservoir characterization of the Paleogene Khurmala Formation in Tawke and Shaqlawa areas, Kurdistan Region of Iraq", *Iraqi Geological Journal***,** vol. 57, no. 1C, pp. 62-77, 2024. https://doi.org/10.46717/igj.57.1C.5ms-2024-3-17

[17] M. Rider, "The geological interpretation of well logs", 2nd ed., *Sutherland: Rider-French Consulting Ltd*, 2002.

[18] M. Ghorab, A. M. Ramadan, and A. Z. Nouh, "The relation between the shale origin (source or non-source) and its type for Abu Roash Formation at Wadi El-Natrun area, south of Western Desert, Egypt", *Australian Journal of Basic and Applied Sciences*, vol. 2, no. 3, pp. 360–371, 2008.

[19] O. Horsfall, V. Omubo-Pepple, and I. Tamunobereton-Ari, "Correlation analysis between sonic and density logs for porosity determination in the south-eastern part of the Niger Delta Basin of Nigeria", *Asian Journal of Science and Technology*, vol. 4, no. 3, pp. 1-5, 2013.

[20] F. K. North, "Petroleum geology", *Boston: Allen amp Unwin*, 607p, 1985.

[21] G.B. Asquith, D. Krygowski, and C.R. Gibson, "Basic well log analysis", *Tulsa: American Association of Petroleum Geologists AAPG*, vol. 16, pp. 305-371, 2004.

[22] D. Tiab and E. C. Donaldson, "Petrophysics: Theory and practice of measuring reservoir rock and fluid transport properties", 4th ed., *Boston: Gulf Professional Publishing*, pp. 260-628, 2015.

[23] Schlumberger, "Log interpretation/charts", *Houston, USA: Schlumberger Wireline and Testing*, 1997.

[24] S. Mohaghegh, B. Balan, and S. Ameri, "Permeability determination from well log data", *SPE formation evaluation*, vol. 12, no. 3, pp. 170-174, 1997. https://doi.org/10.2118/30978-PA